Galileo High Accuracy Service in Real-Time PNT, Geoscience and Monitoring Applications

T. Hadas, K. Kazmierski, I. Kudłacik, G. Marut, and S. Madraszek

***Abstract*— Satellite transmission of orbit and clock corrections is critical for real-time positioning, navigation, and timing (PNT), geoscience applications, safety, and liability critical services based on Global Navigation Satellite Systems (GNSSs) precise positioning. In response to such a demand, Galileo has established a high accuracy service (HAS) of almost global coverage for GPS and Galileo. We validate the quality of HAS corrections and investigate service performance in a variety of applications. Decimeter-level accuracy of HAS corrections leads to static and kinematic positioning with precision of a few centimeters and sub-decimeters, respectively, and timing precision of a single nanosecond. Other GNSS-derived products meet the requirements of real-time GNSS meteorology and allow for monitoring coseismic vibrations. Although other internet correction streams offer superior results, HAS provides better performance than nominal and nearly global coverage.**

***Index Terms*— Earthquakes, Galileo, global navigation satellite systems (GNSSs), high accuracy service, positioning, navigation, and timing (PNT), real-time, remote sensing, troposphere.**

I. Introduction

REAL-TIME precise positioning, navigation, and timing (PNT) with Global Navigation Satellite Systems (GNSSs) for many years was limited to the Real-Time Kinematics (RTK) technique, which allows for achieving an accuracy of a few centimeters but requires a nearby reference station to transmit corrections to observations via radio or internet connection [1]. Worldwide PNT coverage is offered by the Precise Point Positioning (PPP) technique, but the sub-decimeter accuracy requires at least dual-frequency observations and some time, typically minutes to hours, before the solution converges [2]. Real-time PPP has been available since 2013, when the International GNSS Service (IGS) launched the IGS Real-Time Service (RTS, https://igs.org/rts/) with satellite orbit and clock corrections for GPS and GLONASS streamed over the internet. Several IGS analysis centers that contribute to RTS currently support all four GNSS; some of them additionally provide code and phase biases, the latter being a prerequisite for PPP with ambiguity resolution [3].

Manuscript received 23 October 2023; revised 27 December 2023; accepted 10 January 2024. Date of publication 15 January 2024; date of current version 31 January 2024. This research was funded by the National Centre for Research and Development under the LEADER XIII Program, contract No. LIDER13/0075/2022. The article processing charge (APC) was financed by Wrocław University of Environmental and Life Sciences. *(Corresponding author: T. Hadas.)*

The authors are with the Institute of Geodesy and Geoinformatics, Wrocław University of Environmental and Life Sciences, 50357 Wroclaw, Poland (e-mail: tomasz.hadas@upwr.edu.pl; kamil.kazmierski@upwr.edu.pl; iwona.kudlacik@upwr.edu.pl; grzegorz.marut@upwr.edu.pl; szymon.madraszek@upwr.edu.pl).

Digital Object Identifier 10.1109/LGRS.2024.3354293

Although the accuracy of PPP depends, among others, on satellite visibility, length of observation, and receiver dynamics, the accuracy of satellite orbits and clocks directly affects the PPP results. The combined IGS RTS orbits are accurate to 50 mm for GPS and 130 mm for GLONASS. The corresponding values for clocks are 0.3 and 0.8 ns [4]. Over the last decade, together with the major evolution of GNSS, like the development of Galileo and BeiDou constellations, the accuracy of real-time products has been improved. Nevertheless, their quality is heterogeneous across different systems and satellite types. The signal in space range error (SISRE) [5] varies from 16 mm for Galileo, through 23 mm for GPS, and exceeds 50 mm for GLONASS and BeiDou [6].

A variety of geoscience applications exploiting real-time PPP has been demonstrated. The technique supports robust and accurate navigation for unmanned aerial vehicles [7]. It has proved to be useful for highly dynamic airplane flights, providing accuracy at the level of 0.20–0.30 m [8], whereas a sub-decimeter accuracy is achievable for in-land autonomous driving in the urban environment [9] and vessel navigation [10]. PPP is demanded in precision agriculture applications, in which centimeter-level precision is demonstrated under open-sky conditions [11]. The technique is also used as an all-weather tool for water vapor monitoring, providing performance that legitimates the assimilation of troposphere products from GNSS into numerical weather models [12]. Due to its low cost and no reference station required, PPP is directly applicable to a large area and slow-variable landslide monitoring [13]. Sub-cm land deformations in the mining areas are detectable [14]. Coseismic displacement waveforms are retrieved with horizontal and vertical accuracies of 1.2 and 2.4 cm, respectively [15]. Time transfer uncertainty with real-time PPP is better than 0.3 ns [16].

Despite the great potential of the real-time PPP technique, temporal unavailability of real-time corrections, i.e., due to internet disconnections, prevents from providing continuous results. Therefore, real-time PPP has not been operationally implemented in safety or liability critical systems such as natural hazard monitoring, aviation, or time transfer. To overcome this limitation, orbit and clock corrections need to be transmitted via a reliable medium, e.g., satellite link. The first high-precision signal has been transmitted by the Japanese Centimeter Level Augmentation Service (CLAS) since 2018, providing centimeter-level positioning accuracy within the service area of Japan [17]. Since 2020, PPP-B2b has been provided by BeiDou geosynchronous satellites and

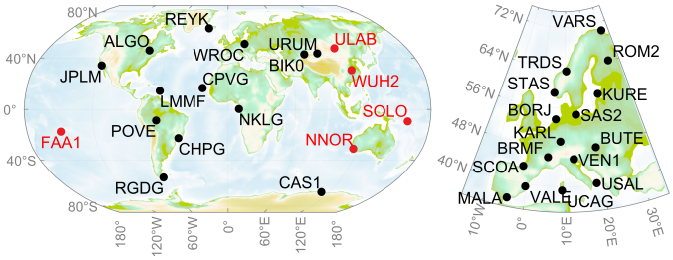

Fig. 1. Distribution of test stations from (left) IGS and (right) EPN networks; stations outside the HAS service area are marked with red.

supports GPS and BeiDou satellites [18]. It provides a decimeter-level kinematic positioning for users located in the Asia-Pacific area [19]. In 2024, the Quasi-Zenith Satellite System (QZSS) will start transmitting MADOCA-PPP service [20], supporting all GNSS, but also limiting to the Asia-Pacific area (https://qzss.go.jp). Since February 2023, Galileo high accuracy service (HAS) has offered almost global coverage (excluding some Asia-Pacific regions) for GPS and Galileo [21]. The GPS and Galileo solution using test signals from 2022 indicated SISRE of 10–12 cm, and positioning accuracy of 13 cm horizontally, and 19 cm vertically at the 95th percentile [22]. The performance of HAS corrections and PPP positioning results is confirmed [23], [24]. Although HAS was designed for PPP, it improves also standard code-based positioning [25]. Currently, validation of Galileo HAS in other geoscience applications has not been conducted.

In this letter, we evaluate the quality of orbit and clock corrections provided by the Galileo HAS. Moreover, we investigate service performance in selected real-time GNSS applications, i.e., static positioning, navigation, timing, remote-sensing of water vapor content in the troposphere, and coseismic vibrations monitoring.

II. Methods

A. Data and Products

The test period covers 68 days, i.e., from the 33rd to the 100th day of the year (DoY), 2023. Observation data come from worldwide distributed stations [see Fig. 1] among which 18 and 16 belong to the IGS network and European Permanent Network (EPN), respectively. Five IGS stations are outside the HAS service area. Seven stations are included in the IGS Final clock products. All selected stations track GPS and Galileo and provide a real-time observation stream. High-rate (HR) GNSS observations from seven stations used for the earthquake experiment come from TUSAGA-Active System (https://www.tusaga-aktif.gov.tr/).

Reference coordinates for all stations are estimated on a daily basis using the online CSRS-PPP service [26]. Zenith total delay (ZTD) final products are provided by: 1) the United States Naval Observatory (USNO) for IGS stations; 2) the Center of Orbit Determination in Europe (CODE) for IGS stations; and 3) selected EPN analysis centers for EPN stations. The interval is 5 min, 2 h, and 1 h, respectively. Seismological data are provided by the Turkish Earthquake Data Center.

B. GNSS Processing Strategy

The in-house developed software is used to process GPS and Galileo undifferenced and uncombined observations with the PPP technique [27] and applies real-time corrections decoded by the BKG NTRIP Client (BNC) v2.12.18 software (https://igs.bkg.bund.de/ntrip/bnc). A detailed description of the PPP model and strategy is provided in [12]. Two streams are used, i.e., 1) SSRA00EUH0 (HAS) available at the ntrip.gsc-europa.eu caster, which contains Galileo HAS corrections; and 2) SSRA00CNE0 (CNS) available at the products.igs-ip.net caster, whose accuracy and performance have been already evaluated in detail [28]. Such an approach allows for a fair comparison of the quality of real-time results obtained through the application of Galileo HAS corrections.

The Galileo HAS orbit corrections are composed of satellite-specific radial (ε_N), in-track (ε_T), and cross-track (ε_W) components. The satellite clock corrections are composed of satellite-specific Delta Clock Correction (δC^s_C) and a system-specific Delta Clock Multiplier (δC^s_M). After determining the position (x^s), velocity ($\dot{x}^s$), and clock error (dt^s) of the satellite s using the Galileo I/NAV broadcast message that matches the issue of data (IOD), the corrected satellite position ($\tilde{x}^s$) and clock offset ($\tilde{dt}^s$) are computed [29]

$$\tilde{x}^s = x^s + \begin{bmatrix} e_N & e_T & e_W \end{bmatrix} \cdot \begin{bmatrix} \varepsilon_N & \varepsilon_T & \varepsilon_W \end{bmatrix}^T \quad (1)$$

$$\tilde{dt}^s = dt^s - \frac{2x^s \cdot \dot{x}^s}{c^2} + \frac{\delta C^s_C \cdot \delta C^s_M}{c} \quad (2)$$

with

$$e_T = \dot{x}^s / \left|\dot{x}^s\right| \quad (3)$$

$$e_W = \left(x^s \times \dot{x}^s\right) / \left(\left|x^s \times \dot{x}^s\right|\right) \quad (4)$$

$$e_N = e_T \times e_W \quad (5)$$

where $c = 299792458.0$ m/s is the speed of light.

III. Results

A. Quality of Corrections

As the indicator of product quality, we use the SISRE parameter, which reflects the impact of satellite orbit and clock quality, directly affecting the PPP results. The SISRE values for the CNS and HAS streams are determined relative to the CODE final product [see Fig. 2] following the procedure described in [5]. Since both real-time streams refer to the satellite antenna phase center (APC), while the Final product contains the satellite's center of mass (CoM) coordinates, we use igs20.atx calibration for GPS and official metadata calibration for Galileo (https://www.gsc-europa.eu/support-to-developers/galileo-satellite-metadata) to transform real-time coordinates from APC to CoM. For HAS, the average SISRE was 8.6 and 13.0 cm for GPS and Galileo respectively. For CNS, both SISREs are reduced by more than half. It should be noted that HAS quality remains almost constant over time, whereas CNS SISRE, especially for Galileo, changes significantly day by day.

B. Static and Kinematic Positioning

We compare daily static coordinates estimated with HAS and CNS with the daily static CSRS-PPP solutions [see Fig. 3].

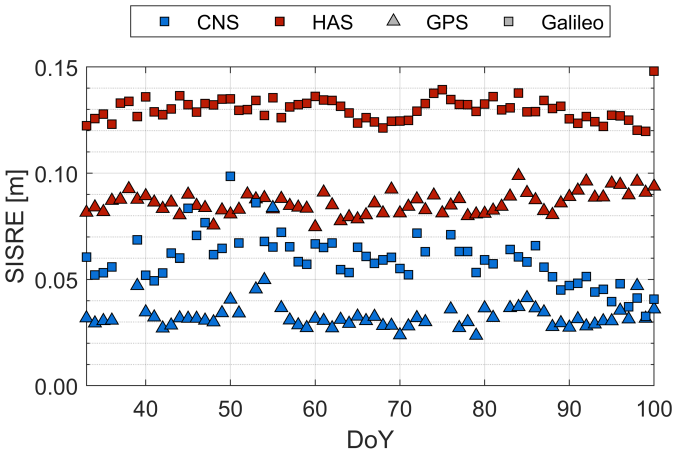

Fig. 2. Daily SISRE for GPS and Galileo satellites calculated with CNS and HAS real-time products.

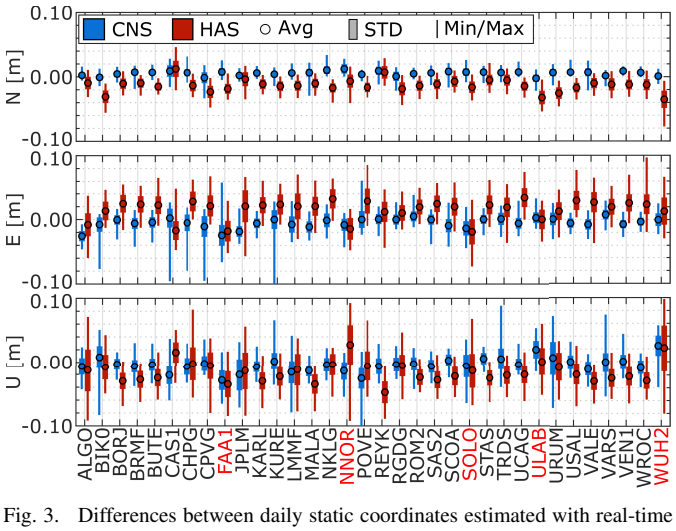

Fig. 3. Differences between daily static coordinates estimated with real-time streams and reference coordinates of stations.

Station-specific offsets obtained with HAS vary from +1 to +102 mm and from −92 to +98 mm for the horizontal and vertical components, respectively. The corresponding ranges for CNS are from 0 to +101 mm, and from −128 to +88 mm. For HAS, the average standard deviations of differences are 18 mm and 19 mm for the horizontal and vertical components, respectively, while for CNS the precision is c.a. 1.5 times better, i.e., 11 mm horizontally and 13 mm vertically. We found no significant degradation of results for stations located outside the HAS service area, except for the vertical component, for which stations WUH2 and NNOR reveal lower precision.

In the kinematic mode [see Fig. 4], reflecting a navigation scenario, each epoch solution is subtracted from the reference coordinates. The station-specific offsets remain at a few cm level for CNS and HAS solutions. Moreover, the precision of both solutions is similar, i.e., 91 and 93 mm in the horizontal component, for CNS and HAS, respectively; and 106 and 118 mm in the vertical component, respectively. Such results indicate that in the kinematic mode, the lower accuracy of corrections is not a main limiting factor, thus the results obtained with HAS are of comparable quality to precise positioning obtained with other corrections streams.

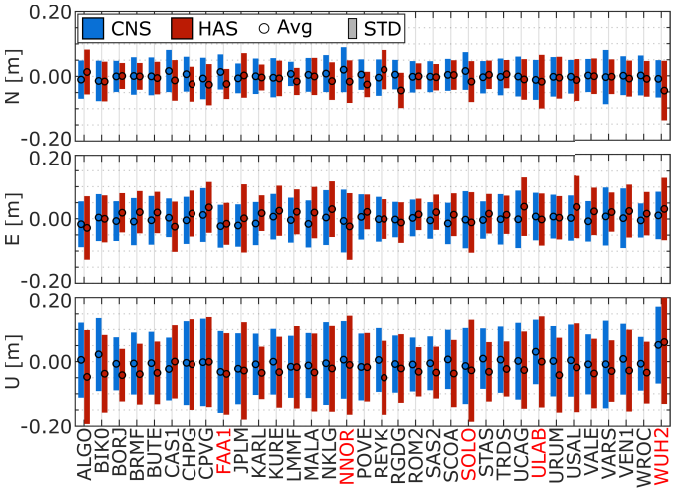

Fig. 4. Differences between kinematic coordinates estimated with real-time streams and reference coordinates of stations.

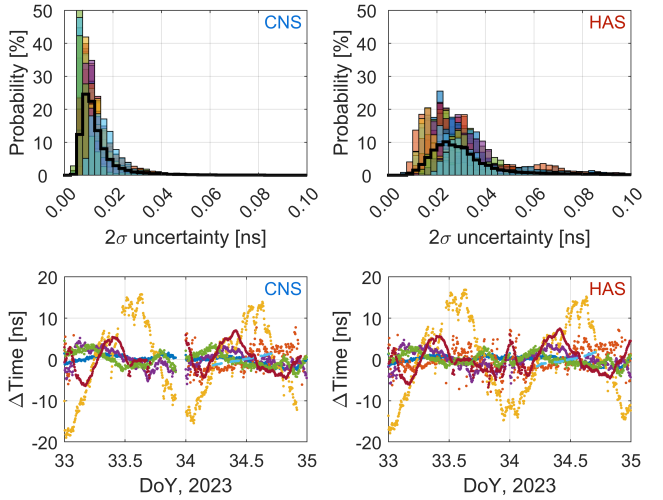

Fig. 5. Timing (top) uncertainty (95% confidence level) and (bottom) precision with (left) CNS and (right) HAS corrections; color lines represent individual station and black lines represent overall results.

C. Timing

Although the estimated uncertainty, i.e., a posteriori error of receiver clock offset estimates varies among stations [see Fig. 5(a) and (b)], it is significantly lower for the CNS solution than for the HAS solution. For the 95% confidence level, the uncertainty is 0.03 and 0.06 ns, respectively. Neglecting the first 3 h, considered as the PPP initialization period, the extreme values are 0.08 and 0.10 ns, for CNS and HAS, respectively. It should be noted that the provided uncertainties are over-optimistic, which is typical for long-term PPP solutions employing the Kalman filter approach.

We analyze the timing accuracy and precision for stations ALGO, CPVG, FAA1, LMMF, NKLG, NNOR, and POVE, which are included in the IGS Final clock product [see Fig. 5(c) and (d)]. The test stations are equipped with geodetic-grade hardware, but none has been calibrated for timing applications by a timing laboratory. Therefore, due to site-specific hardware biases and alternative GNSS data processing technique, i.e., double-differencing, utilized by the IGS, the estimated receiver clock errors differ from the IGS Final clock product [30]. With CNS corrections, the

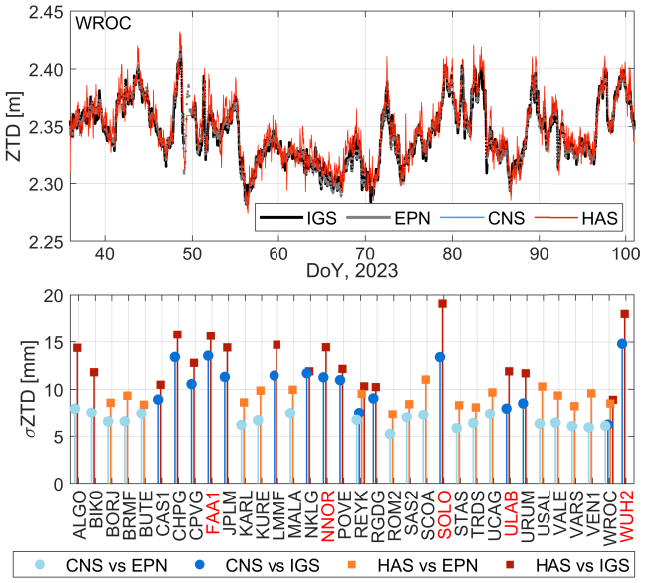

Fig. 6. Comparison of ZTD obtained with CNS and HAS against Final products from EPN and IGS. (Top) time series for station WROC. (Bottom) standard deviation of differences.

extreme biases, i.e., the mean difference between estimates and reference is −88.8 ns for station FAA1 and +88.4 ns for station NNOR, whereas for the other five stations they vary from −8.7 to −0.8 ns. The biases estimated with CNS are smaller by 0.5 to 1.5 ns, except for station FAA1, for which the bias is larger by 2.4 ns. The precision, reflected by the standard deviation of differences between estimates and reference, varies from 0.8 to 3.3 ns with HAS and from 0.9 to 3.3 ns with CNS, except for station FAA1, for which the corresponding precision is 9.4 and 9.0 ns. Interestingly, the precision obtained with both real-time streams agrees to 0.3 ns and is typically better with HAS than with CNS.

D. Troposphere Monitoring

We obtain an almost continuous solution for ZTD [see Fig. 6(a)]. Individual gaps occur only during a misperformance of stations, which results in corresponding discontinuities in the final products. Both real-time solutions are well aligned with the IGS and the EPN Final product. Although we notice individual peaks in the CNS solution, in most cases, the HAS solution is noisier than the CNS solution. This is further confirmed by the analysis of the ZTD precision among all stations [see Fig. 6(b)]. For all EPN stations, the standard deviation of differences between the real-time CNS solution and the EPN Final product remains below 8 mm, whereas for the HAS solution, the precision is better than 11 mm. The corresponding numbers for IGS stations with respect to the IGS Final product are 15 and 19 mm. We notice that three out of four stations, for which the precision against the IGS Final products exceeds 15 mm, i.e., FAA1, SOLO, and WUH2, are outside the HAS service area. Nevertheless, the average ZTD accuracy of 9 and 14 mm is reached with HAS for EPN and IGS stations, respectively, which is still below the threshold (15 mm) and target (10 mm) accuracy of ZTD products for NWP assimilation [31].

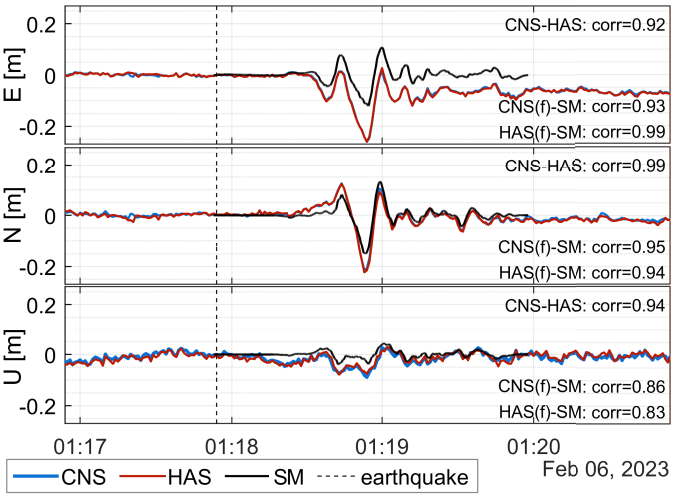

Fig. 7. HR GNSS displacements compared to SM solution (TUF1/0129), earthquake M7.7, Turkey. For correlation with SM, the HR GNSS is filtered.

E. Coseismic Vibrations Monitoring

We validate the short-term performance of HR GNSS as the unbiased root mean square error (RMSE) for undisturbed scenarios, i.e., within 120 s before an earthquake, as PPP typically delivers higher accuracy for shorter periods, outperforming longer durations [32]. The accuracy of displacements obtained with CNS corrections is 12 mm horizontally and 25 mm vertically, while the accuracy of time series acquired with HAS corrections is slightly inferior, measuring 20 mm horizontally and 46 mm vertically. Nonetheless, denoising is necessary for the HR GNSS time series to reliably assess earthquake-induced vibrations due to low-frequency noise [33]. To this end, both time series are subjected to high-pass filtering with a cutoff frequency of 0.01 Hz. The median Pearson's correlation values for horizontal components obtained with CNS and HAS corrections, in reference to the seismic solution (SM), are nearly identical, at 0.85 and 0.84, respectively. However, a noticeable difference is observed in the correlation of the Up component, with values of 0.72 for CNS and 0.60 for the HAS solution. Although CNS and HAS solutions show great agreement for East and North components with correlation coefficients equal to 0.99, they differ for the vertical component [see Fig. 7].

IV. Conclusion

The Galileo HAS real-time orbit and clock corrections are continuously provided via a globally available satellite link and their accuracy is close to well-established state-of-the-art internet correction streams. We confirm that the performance of the PPP solution with HAS is better than nominal, with minor degradation for stations located outside the service area. Although in some precise geoscience applications, such as static positioning and troposphere monitoring, the results are not as good as with the CNS stream, they still meet the target requirements from corresponding communities. Therefore, HAS offers a great alternative for internet streams and it is expected, that new real-time GNSS-based geoscience applications, including safety and liability critical services, will appear and improve soon.

ACKNOWLEDGMENT

The authors would like to thank EUSPA and CNES for streaming real-time corrections, and NRC for providing the CSRS-PPP service. The IGS, EPN, USNO, CODE, TUSAGA-Active System, and Turkish Earthquake Data Center for sharing GNSS observations and products.

REFERENCES

[1] C. Rizos, "Network RTK research and implementation: A geodetic perspective," *J. Global Positioning Syst.*, vol. 1, no. 2, pp. 144–150, Dec. 2002, doi: 10.5081/jgps.1.2.144.

[2] A. B. Anquela, A. Martín, J. L. Berné, and J. Padín, "GPS and GLONASS static and kinematic PPP results," *J. Surveying Eng.*, vol. 139, no. 1, pp. 47–58, Feb. 2013, doi: 10.1061/(asce)su.1943-5428.0000091.

[3] M. Glaner and R. Weber, "PPP with integer ambiguity resolution for GPS and Galileo using satellite products from different analysis centers," *GPS Solutions*, vol. 25, no. 3, p. 102, May 2021, doi: 10.1007/s10291-021-01140-z.

[4] T. Hadas and J. Bosy, "IGS RTS precise orbits and clocks verification and quality degradation over time," *GPS Solutions*, vol. 19, no. 1, pp. 93–105, Feb. 2014, doi: 10.1007/s10291-014-0369-5.

[5] O. Montenbruck, P. Steigenberger, and A. Hauschild, "Multi-GNSS signal-in-space range error assessment—Methodology and results," *Adv. Space Res.*, vol. 61, no. 12, pp. 3020–3038, Jun. 2018, doi: 10.1016/j.asr.2018.03.041.

[6] K. Kazmierski, R. Zajdel, and K. Sośnica, "Evolution of orbit and clock quality for real-time multi-GNSS solutions," *GPS Solutions*, vol. 24, no. 4, p. 111, Oct. 2020, doi: 10.1007/s10291-020-01026-6.

[7] C. Chi, X. Zhan, S. Wang, and Y. Zhai, "Enabling robust and accurate navigation for UAVs using real-time GNSS precise point positioning and IMU integration," *Aeronaut. J.*, vol. 125, no. 1283, pp. 87–108, Oct. 2020, doi: 10.1017/aer.2020.80.

[8] J. F. G. Monico et al., "Real time PPP applied to airplane flight tests," *Boletim de Ciências Geodésicas*, vol. 25, no. 2, Jul. 2019, Art. no. e2019009, doi: 10.1590/s1982-21702019000200009.

[9] V. Ilçi and A. U. Peker, "The kinematic performance of real-time PPP services in challenging environment," *Measurement*, vol. 189, Feb. 2022, Art. no. 110434, doi: 10.1016/j.measurement.2021.110434.

[10] R. M. Alkan, S. Erol, V. Ilçi, and M. Ozulu, "Comparative analysis of real-time kinematic and PPP techniques in dynamic environment," *Measurement*, vol. 163, Oct. 2020, Art. no. 107995, doi: 10.1016/j.measurement.2020.107995.

[11] J. Guo et al., "Multi-GNSS precise point positioning for precision agriculture," *Precis. Agricult.*, vol. 19, no. 5, pp. 895–911, Mar. 2018, doi: 10.1007/s11119-018-9563-8.

[12] T. Hadas, T. Hobiger, and P. Hordyniec, "Considering different recent advancements in GNSS on real-time zenith troposphere estimates," *GPS Solutions*, vol. 24, no. 4, p. 9, Jul. 2020, doi: 10.1007/s10291-020-01014-w.

[13] G. Huang, S. Du, and D. Wang, "GNSS techniques for real-time monitoring of landslides: A review," *Satell. Navigat.*, vol. 4, no. 1, p. 5, Feb. 2023, doi: 10.1186/s43020-023-00095-5.

[14] D. Tondas, K. Kazmierski, and J. Kaplon, "Real-time and near real-time displacement monitoring with GNSS observations in the mining activity areas," *IEEE J. Sel. Topics Appl. Earth Observ. Remote Sens.*, vol. 16, pp. 5963–5972, 2023, doi: 10.1109/JSTARS.2023.3290673.

[15] Y. Zhang, Z. Nie, Z. Wang, H. Wu, and X. Xu, "Real-time coseismic displacement retrieval based on temporal point positioning with IGS RTS correction products," *Sensors*, vol. 21, no. 2, p. 334, Jan. 2021, doi: 10.3390/s21020334.

[16] X. Wang, F. Shi, L. Zhao-nan, and Y. Jin, "The method of real-time PPP time transfer research," *IOP Conf. Ser., Earth Environ. Sci.*, vol. 310, no. 2, Aug. 2019, Art. no. 022030, doi: 10.1088/1755-1315/310/2/022030.

[17] Y. Zhang, N. Kubo, and S. Pullen, "Evaluation of QZSS centimeter level augmentation system (CLAS): Open-sky to urban environments and geodetic to low-cost receivers," in *Proc. I_{ON} GNSS+, Int. Tech. Meeting Satell. Division Inst. Navigat.*, Oct. 2022, pp. 2729–2750, doi: 10.33012/2022.18517.

[18] (Jul. 2020). *BeiDou Navigation Satellite System Signal In Space Interface Control Document: Precise Point Positioning Service Signal PPP-B2b, China Satellite Navigation Office*. [Online]. Available: http://en.beidou.gov.cn/SYSTEMS/ICD/202008/P020200803538771492778.pdf

[19] P. Wu et al., "Evaluation of real-time kinematic positioning performance of the BDS-3 PPP service on B2b signal," *GPS Solutions*, vol. 27, no. 4, p. 192, Aug. 2023, doi: 10.1007/s10291-023-01532-3.

[20] K. Kawate et al., "MADOCA: Japanese precise orbit and clock determination tool for GNSS," *Adv. Space Res.*, vol. 71, no. 10, pp. 3927–3950, May 2023, doi: 10.1016/j.asr.2023.01.060.

[21] (Jan. 2023). *Galileo High Accuracy Service–Service Definition Document (HAS SDD)*. European Union. [Online]. Available: https://www.gsc-europa.eu/sites/default/files/sites/all/files/Galileo-HAS-SDD_v1.0.pdf

[22] N. Naciri, D. Yi, S. Bisnath, F. J. de Blas, and R. Capua, "Assessment of Galileo high accuracy service (HAS) test signals and preliminary positioning performance," *GPS Solutions*, vol. 27, no. 2, p. 73, Feb. 2023, doi: 10.1007/s10291-023-01410-y.

[23] C. Parra, A. Schütz, U. Hugentobler, T. Pany and S. Baumann, "The Galileo high-accuracy service: Evaluating the quality of the corrections and initial PPP performance," *Eng. Proc.*, vol. 54, no. 1, p. 14, Oct. 2023, doi: 10.3390/ENC2023-15450.

[24] I. Martini, M. Susi, L. Cucchi, and I. Fernandez-Hernandez, "Galileo high accuracy service performance and anomaly mitigation capabilities," *GPS Solutions*, vol. 28, no. 1, p. 25, Jan. 2024, doi: 10.1007/s10291-023-01555-w.

[25] A. Angrisano, S. Ascione, G. Cappello, C. Gioia, and S. Gaglione, "Application of 'galileo high accuracy servic, on single-point positioning," *Sensors*, vol. 23, no. 9, p. 4223, Apr. 2023, doi: 10.3390/s23094223.

[26] (Aug. 2020). *CSRS-PPP Version 3: Tutorial, Natural Resources Canada, Canada*. [Online]. Available: https://webapp.csrs-scrs.nrcan-rncan.gc.ca/geod/tools-outils/sample_doc_filesV3/NRCan

[27] E. Schönemann, "Analysis of GNSS raw observations in PPP solutions," Ph.D. dissertation, Fachbereich Bau-und Umweltingenieurwissenschaften, Technische Universität, Darmstadt, Germany, May 2014. Accessed: May 18, 2023.

[28] K. Kazmierski, K. Sośnica, and T. Hadas, "Quality assessment of multi-GNSS orbits and clocks for real-time precise point positioning," *GPS Solutions*, vol. 22, no. 1, p. 11, Jan. 2018, doi: 10.1007/s10291-017-0678-6.

[29] (May 2022). *Galileo High Accuracy Service Signal-In-Space Interface Control Document (HAS SIS ICD)*. European Union. [Online]. Available: https://www.gsc-europa.eu/sites/default/files/sites/all/files/Galileo_HAS_SIS_ICD_v1.0.pdf

[30] L. Carlin, O. Montenbruck, J. Furthner, and A. Hauschild, "UTC and GNSS system time access using PPP with broadcast ephemerides," *GPS Solutions*, vol. 26, no. 4, p. 142, Oct. 2022, doi: 10.1007/s10291-022-01326-z.

[31] N. Dymarska et al., "An assessment of the quality of near-real time GNSS observations as a potential data source for meteorology," *Meteorol. Hydrol. Water Manage.*, vol. 5, no. 1, pp. 3–13, Jan. 2017, doi: 10.26491/mhwm/65146.

[32] Y. Shu, Y. Shi, P. Xu, X. Niu, and J. Liu, "Error analysis of high-rate GNSS precise point positioning for seismic wave measurement," *Adv. Space Res.*, vol. 59, no. 11, pp. 2691–2713, Jun. 2017, doi: 10.1016/j.asr.2017.02.006.

[33] I. Kudlacik, "Seismic phenomena in tke light high-rate GPS precise point positioning results," *Acta Geodynamica et Geomaterialia*, vol. 16, no. 1, pp. 99–112, Mar. 2019, doi: 10.13168/agg.2019.0008.